RESEARCH PAPER

Assessment of Structure, Dielectric and Gamma-Shielding Properties of Chemically Treated Natural Kaolinite Clay

Anas Yousef Al-Reyahi[1], Yahya Salem Al-Degs[2,*], Ayman Abdulla Issa[2], Ziad yousef khattari[1], Mohammed Abu Al Sayyed[3]

* *yahya@hu.edu.jo*

[1] Department of Physics, Faculty of Science, The Hashemite University, Zarqa, Jordan.
[2] Department of Chemistry, Faculty of Science, The Hashemite University, Zarqa, Jordan.
[3] Faculty of Science, University of Tabuk, Saudi Arabia

Received: January 2021 **Revised: July 2021** **Accepted: August 2021**
DOI: 10.22068/ijmse.2114

Abstract: *The structural properties of a natural clay sample (51% kaolinite) were tailored to suit specific applications. H_2SO_4 and NaOH (1.0 M) treatment caused structural alterations and a significant release of Al ions compared to Si ions. Chemical treatment caused structural alterations, according to XRD analysis. FTIR analysis also indicated higher density of polar surface groups upon treatment which affected the corresponding dielectric behavior. Dielectric measurements showed their suitability in the frequency dependent dialectical insulator applications. Acid treated kaolinite was a promising dielectric at 10 and 1000 Hz. With appropriate mass attenuation coefficients (μ/ρ) of 12.098-12.182 cm^2/g and a high half value layer of 10 cm at 10 keV, kaolinite and other treated forms were adequate to act shielding material.*

Keywords: *Kaolinite, Acid/alkali treatment, Physicochemical characteristics, Dielectric and shielding properties.*

1. INTRODUCTION

Clay minerals' physicochemical features have been extensively studied by various researchers due to their unusual adsorption, dielectrical, and catalytic capabilities. [1-4]. Such behaviors are often controlled by surface area, porosity and surface chemistry which is often modified by different treatment procedures [4]. The physicochemical properties of clay minerals are adjusted by two main modification procedures [4, 5]: (A) physical modification, such as thermal treatment in conventional ovens or microwaves, which results in changes to the crystalline or textual structure and surface chemistry, and (B) chemical treatment with appropriate materials, such as strong acids/bases and organic compounds, which can change textural properties (crystallinity, specific surface area and pore volume) and distribution of surface functional groups [6-7]. In fact, the common physical treatment is often accomplished by direct thermal treatment which impacts chemical composition and crystalline structure by the action of high temperature [8]. In some cases, mineralogy, cation exchange capacity, swelling properties, specific surface area/porosity, particle size, acidity, dielectrical properties and catalytic activity would be adjusted by thermal or microwave treatment [9, 10]. Combination of heat and chemical treatments was also tested to get better adsorption and catalytic activity of clay minerals [4, 8]. Acid or alkali attack induces marked changes in the crystal structure of aluminosilicate minerals due to dissolution of structural ions and/or rearrangement of the structure [4-7]. Superior specific surface area, porosity, and acidic sites were obtained after acid treatment of bentonite, montmorillonite, kaolin, and vermiculite, which is appealing for many practical applications [11]. Kaolinite was exposed to H_2SO_4 and microwave heating at 600 W in a recent work [10]. Significant physicochemical changes were observed upon treatment and modified clay manifested better adsorption for tartrazine dye due to improvements in textural and chemical properties [10]. Beside improvements in surface area and porosity, the dielectrical parameters including dielectric constant, dielectric loss factor, and AC-conductivity were notably affected upon acid treatment of clay material [10]. Although strong acids are common clay-activators, several practical problems were reported when using acid-modified-clay for refining oil products which resulted in corrosion of the process vessels, production of higher levels of free fatty acids, and leading to higher peroxide value [12].

[Downloaded from aed.iust.ac.ir on 2025-04-14]

[DOI: 10.22068/ijmse.2114]

Accordingly, cationic and anionic surfactants modifiers were suggested to uptake of free fatty acids and peroxides produced upon using acid-modified-clay [13]. In fact, testing other materials including organic acids and strong bases was reported toward certain applications [12, 13].

On the other hand, alkali treatment of aluminosilicates has been investigated by many researchers and the aims behind surface treatment are: a) conversion of clay minerals to strong, water resistant, and durable product which will permit the manufacture of concrete block replacements [14, 15], b) phase transformation of certain minerals into structurally different minerals like zeolite [16], and c) under mild treatment conditions, surface area and porosity of certain clay minerals can be improved by alkali solutions without serious structural change [4, 5]. Due to its lower energy cost, alkali-modified–clay has been claimed to be an excellent option for Portland cement-based concrete [14]. Clays can also be employed as primary aluminosilicate precursors for geopolymer production [15]. Alkali treatment of montmorillonite, illite, and kaolinite as ingredients for geopolymers were reported [17]. For a reactive aluminosilicate in geopolymer, a Si/Al molar ratio of 1.5 –2.5 is necessary in addition to concentrated alkali medium [18]. Kumar and co-workers have been tested acids and bases to activate/modify kaolin at mild conditions and the results suggested that NaOH is a good substitute for HCl to generate high surface area and porosity of the treated material with slight changes in the infrastructure [19]. In a systematic study, Belver and co-workers have investigated on the effect of strong acids and bases on the chemical and textural properties of kaolin [6]. In fact, kaolin treatment is dependent on the type, concentration, reaction time, and calcination temperature [6]. For acid modification, the best results were reported for reported for HCl (6.0 M) at 90°C and 6 hours treatment time [6]. It seems that NaOH was not promising as the surface area and porosity was not highly changed upon treatment and conversion to zeolite was detected at high concentration of NaOH [6].

Recently, there is more interest to use modified clays as dielectric materials and radiation absorbents [20, 21]. Solid materials (either natural or synesthetic ones) are classified based on their intrinsic electrical characteristics as conductors, semiconductors, super-conductors and insulators [22]. Among measured dielectrical parameters, the electrical conductivity is the most informative as it reflects the ease of charge flow through a medium [22]. Electrons, ions, and charged holes are all accounted for the overall electrical conductivity of solid materials [23]. Clay minerals containing variable amounts of transition metals and upon treatment the dielectric properties should be investigated to check their usage as semiconductors [20, 23]. Radiation shielding is another promising application of clay minerals and other materials which need more investigations [24-35]. In fact, radiation shielding material have been an active research line in nuclear, radiation physics, and radiation protection [24]. Mass attenuation coefficients and half value layer are the most significant parameters that assessed the radiation-shielding performance of solid materials [24-26].

In the current study, a natural kaolinite sample will be activated by different solutions to assess the final practical applications. Both H_2SO_4 and NaOH (1.0 M) will be tested at 110°C for kaolinite modification. X-ray diffraction, X-ray fluorescence, scanning electron microscopy, FTIR, and dielectrical and radiation shielding qualities are among the characterisation tests. The outcomes of the characterisation tests will be used to evaluate the practical uses of raw and various processed forms.

2. MATERIALS AND METHODS

2.1. Natural kaolinite sample

A kaolinite-rich clay sample was donated by the Royal Scientific Society (Amman, Jordan). The clay sample (2 kg) was crushed, sieved to particle size < 45 μm, and washed with distilled water to remove soluble impurities. XRF analysis indicated the followings: SiO_2 48.85%, Al_2O_3 23.50%, Fe_2O_3 4.64%, K_2O 0.82%, MgO 3.41%, and CaO 1.77% and LOI 18.28. Minerals were identified using the EVA software. The strength of a diagnostic peak multiplied by a correction factor was used to assess the semi-quantitative mineralogical composition of bulk powder [36]. Semi-quantitative measurement of the clay fractions was carried out using the approach provided by Moore and Reynolds [36]. All measurements related to mineralogy of clay sample were carried out at Royal Scientific

[Downloaded from aed.iust.ac.ir on 2025-04-14]

[DOI: 10.22068/ijmse.2114]

Society (Amman, Jordan).

2.2. Chemical treatment of clay sample

Chemical treatment step was carried out by adding 10-20 g of dried sample to 150 ml (1.0 M) solution of H_2SO_4 and NaOH and refluxing at 110°C in a round bottomed flask connected to a reflux condenser for three hours. The resulting mixture was cooled and the content was filtered and washed with distilled water to remove any excess reagent, heated at 400°C for two hours, and finally ground to particle size less than 45 µm. In the manuscript, the natural sample is defined as KAO and treated forms are indicated by KAO-H_2SO_4 and KAO-NaOH. The treatment conditions were selected to avoid any serious structural changes in the sample which known to occur at higher concentrations of acids/bases and higher temperatures [37].

2.3. Characterization of activated clay

2.3.1. XRD, XRF, SEM, and FTIR

Structural changes upon chemical treatment were monitored by running X-Ray Diffraction XRD, X-Ray Fluorescence spectroscopy XRF, and Scanning Electron Microscopy (SEM). XRF was carried out using Shimadzu XRF-1800 Sequential X-Ray Fluorescence Spectrometer (Shimadzu, Japan) with a current 40 mA and voltage 40 mV. XRD was performed using Shimadzu X-Ray Diffractometer (Shimadzu X-Ray Diffractometer XRD-6000, Japan). Using XRF, the loss on ignition (LOI) content of the clay sample was contributed to the release of water and estimated by calcinations at 975°C. After calcination, the sample mixed with lithium-tetraborate and lithium iodide and finally fused and moulded to get a glass disk prior to chemical analysis. The patterns were recorded over the range 2θ of 2–60° with a scanning rate of 2°/min. SEM pictures were collected at different magnifications using Inspect F50 (FEI Company, Eindhoven, Netherlands). Before measurements, clay particles were coated using a sputter coater (Quorum Technology, Emitech K550 X, England). Interferometer-AVI (Bruker, USA) spectrometer was used to measure infrared spectra of samples in the range 400-4000 cm^{-1}. At room temperature, samples were placed in a tiny crystal cup (50 mm diameter and 10 mm depth) and measurements were taken.

2.4. Dielectric parameters

Dielectric constant ε', dielectric loss factor ε'' and AC-conductivity σ of samples (over the frequency range 10-106 Hz) were determined by measuring AC impedance at 25°C, using a Solarton-1260 impedance/Gain phase analyser connected to a dielectric interface (Solartron Group Ltd, UK). The capacitance C, the impedance Z and the loss tangent (tan δ) were directly measured and the resulting parameters ε', ε'', and σ were estimated and plotted as a function of applied frequency. Rigid samples of smoothed surfaces were carefully prepared for electrical measurements. 1.0 g of kaolin was compressed under 10 bar to generate a rigid disc of 0.4 mm thickness and 1.0 cm diameter. Solid discs of smooth surface are necessary for good electrical contact and this would ensure stable and consistent results. Before measurement, the disc was carefully coated with Ag past. Dielectric constant ε' was estimated as [38]: $\varepsilon'=Cd/\varepsilon_o a$, where d, a, and ε_o are disc thickness, disc cross-sectional area, and the permittivity of free space, respectively. Dielectric loss factor ε'' was estimated as [38]: $\varepsilon'' = \varepsilon' \tan\delta$ and δ was estimated from phase angle. Finally, AC conductivity was estimated as [38]: $\sigma=\omega\varepsilon_o\varepsilon''$, where ω is the angular frequency which equals $2\pi F$.

2.5. Gamma shielding calculations

The main shielding parameters were estimated from the chemical compositions of solid materials. To measure shielding parameters, several calculation programs were used including XCOM and Xmudat, moreover, Monte Carlo toolkits such as Geant4, MCNP, PHITS, and FLUKA were utilized [25, 27, 30]. The mass attenuation coefficient (μ/ρ, cm^2/g) and the half value layer HVL (cm) were numerically estimated assuming that the amount of absorbed gamma-photons passing a clay sample is following Beer-Lambert's and Bragg`s formulations [24, 25, 30, 39]. More details on estimation of shielding parameters are available in the literature [25, 26, 28-30].

3. RESULTS AND DISCUSSION

3.1. Characterization of kaolinite upon chemical treatment

The changes in the structure of kaolinite after

[Downloaded from aed.iust.ac.ir on 2025-04-14]

[DOI: 10.22068/ijmse.2114]

chemical treatment were investigated using XRD, XRF, SEM, and FTIR techniques.

XRD: The results of XRD and SEM are provided in Figures 1 and 2, respectively. Clay and non-clay minerals such as kaolinite, illite, smectite, quartz, and feldspar were detected using XRD scans. The raw sample (KA) showed the reflections of kaolinite mineral at 2θ of 120, 250 which accounted for the d values of 7.154 Å and reflections from [001]. The peaks appeared at 2θ 6 and 21 evidenced the presence of smectite in the sample. The same scan also evidenced the presence of quartz (2θ 27) and feldspar (2θ 28) as the major non-clay components. Mineralogical investigation revealed that the sample was primarily composed of kaolinite (51%) and smectite (31%), with a little quantity of illite (4 percent).

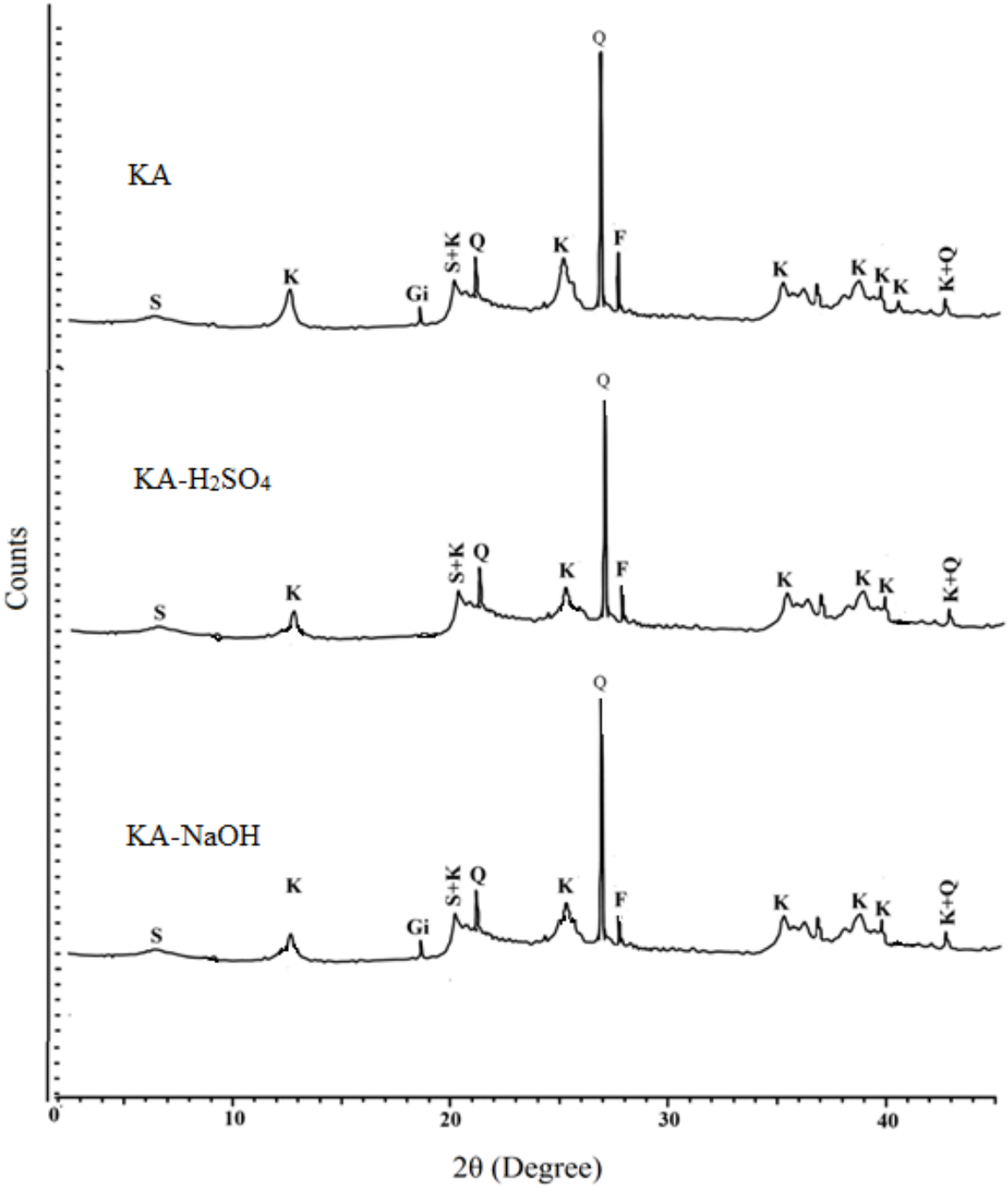

Fig. 1. XRD scans of clay samples. A KAO: B KAO-H_2SO_4: C KAO-NaOH.
S: Smectite; K: Kaolinite; Gi: Gibbsite; Q: Quartz; F-Feldspars

[Downloaded from aed.iust.ac.ir on 2025-04-14]

[DOI: 10.22068/ijmse.2114]

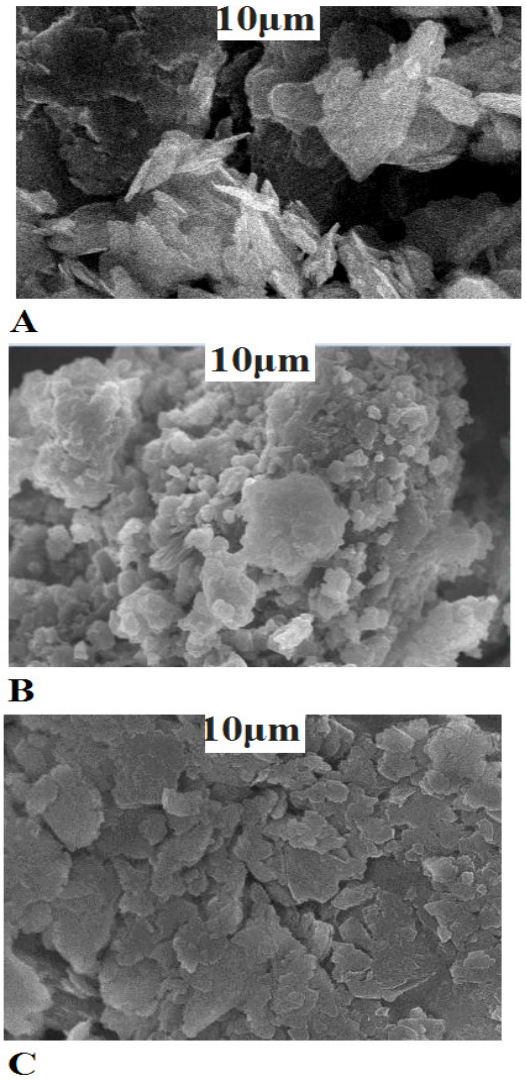

Fig. 2. SEM pictures of clay samples. A KAO: B KAO-H_2SO_4: C KAO-NaOH

Quartz and feldspar accounted for 11 and 2% of the non-clay minerals in the sample, respectively. It was noted that chemical activation causes a decrease in the crystalinity of the sample as indicated from the reduction in the peaks kaolinite (12 and 25 2θ) after treatment (scans 2 and 3). Upon acid treatment, the peak intensities of KA which positioned at 12 and 25 were decreased which attributed to: a) leaching of Al ions, b) structural disorder, and c) deformation of the crystalline character of kaolinite [19, 39]. As a result of structural deformation by acid treatment, the characteristic peak appeared at 12° (accounted for 001 basal plane) was notably reduced after treatment. Gibbsite, which available in a small amount, was removed upon acid treatment. For alkali treatment, a similar XRD scan was generated indicating comparable phase deformation was resulted which mainly attributed to elution of Al cations from the sample. In fact, the high reduction in the intensities of (12° and 25°) peaks strongly reflected the reduction of crystallite size and the decrease of the mean lattice strain in the crystal [19]. After acid and alkali treatment, for example, the decreases in 12° peak were 50 and 56%, respectively. Given the high kaolinite content in the sample, this would imply that significant structural alterations and partial crystal disintegration occurred during treatment (51%).

SEM: The scanning electron micrographs (magnification power ×5000) of all samples are presented in Fig 2. As indicated in Fig 2, the morphological structures of treated kaolinite (Fig 2B and C) were different from the original sample. The existence of big particles, which looked as flaky particles joined together in agglomerates, was shown by SEM micrograph of the raw material. SEM images of acid and alkali treated kaolinite, on the other hand, show morphological differences. For KAO-H_2SO_4, the SEM indicated slight dispersion of the particles into filament, or plate-like fragments. More flaky-particle size decrease was seen with KAO-NaOH, which might be explained by partial dissolution of the silicate mineral into amorphous silica particles.

XRF: XRF analysis was carried out to check chemical composition of original sample and other subsequent changes upon treatment. Table 1 summarizes the results of XRF test along with Si/Al ratios of the samples.

According to XRF analysis, the raw sample has the largest concentrations of alumina and silica, with smaller amounts of iron, calcium, magnesium, and potassium. Clay mineral was present in substantial amounts, as evidenced by the increased mass percentages of silica and alumina. The content of Al_2O_3 was reduced while SiO_2 increased after treatment with both activators. The notable reduction in alumina after treatment was mainly attributed to the leaching of the Al^{3+} ions from inner octahedral layer due to hydrolysis at alkaline and acidic conditions. With the exception of CaO, which was enhanced by NaOH treatment, the contents of Fe_2O_3, K_2O, and MgO were not significantly altered by any reagent. The attacking tetrahedral layer resulted in the de-alumination of clay, which raised the

[Downloaded from aed.iust.ac.ir on 2025-04-14]

[DOI: 10.22068/ijmse.2114]

Si/Al ratio after treatment [19, 40]. Chemical treatment strips octahedral ions including Mg, Al, Fe and removes tetrahedral ions from the clay minerals due to the isomorphous substitution in the crystal lattices. For alkali treatment, NaOH was reported to be aggressive on the sample but at concentration higher than 5.0 M [40].

Table 1. XRF analysis of kaolinitic samples

Oxide%	KA	KA-H_2SO_4	KA-NaOH
SiO_2	48.85	53.76	54.45
Al_2O_3	23.5	19.35	20.04
Fe_2O_3	4.64	5.04	4.88
K_2O	0.82	0.93	0.64
Na_2O	0.11	0.16	0.16
P_2O_5	0.17	0.15	0.16
MgO	0.77	1.04	0.61
CaO	0.88	0.81	1.72
LOI (975°C)	18.28	16.32	15.27
Si/Al ratio	1.77	2.36	2.31
Metals (ppm)	KA	KA-HCl	KA-NaOH
Cr	275.4	295.3	704.6
Mn	196.6	154.4	385.7
Ni	71.8	58.0	86.9

Pentrak and co-workers showed that Si is leached in much higher amounts compared to Al using KOH as activator [39]. All samples are potential ingredients for fabrication of geopolymers as Si/Al ratios were within the range 1.5–2.5 [15].

After alkali treatment, the Cr concentration (mg/kg) increased from 275.4 ppm to 704.6 ppm, as indicated in Table 1. Cr content was similarly elevated with the acid treatment, but to a lesser level. As a result, the basic treatment has increased the amount of Cr (and Mn/Ni) in the final product. The enrichment of Cr was attributed to many surface reactions like precipitation with OH ions or binding with other phases.

FTIR: IR spectra of kaolinite and modified forms are all presented in Figure 3.

For O-H stretching band, KAO shows two bands at 3624 and 3697 cm^{-1} which correspond to Al-OH bond stretching. The 3624 cm^{-1} absorption band is related to the in-phase symmetric stretching vibrations of Al-OH, which are found inside the tetrahedral and octahedral layers. The band at 3697 cm^{-1} is related to the in-phase symmetric stretching vibrations of Al-OH. The attack of the layers that make up the clay was shown by higher band-intensities of 3624 and 3697 cm^{-1} after chemical treatment [6, 19]. The influence of chemical treatment on the structure of clay was evidenced from higher intensity of 3447 cm^{-1} which assigned to the physisorbed water molecules on the surface [39].

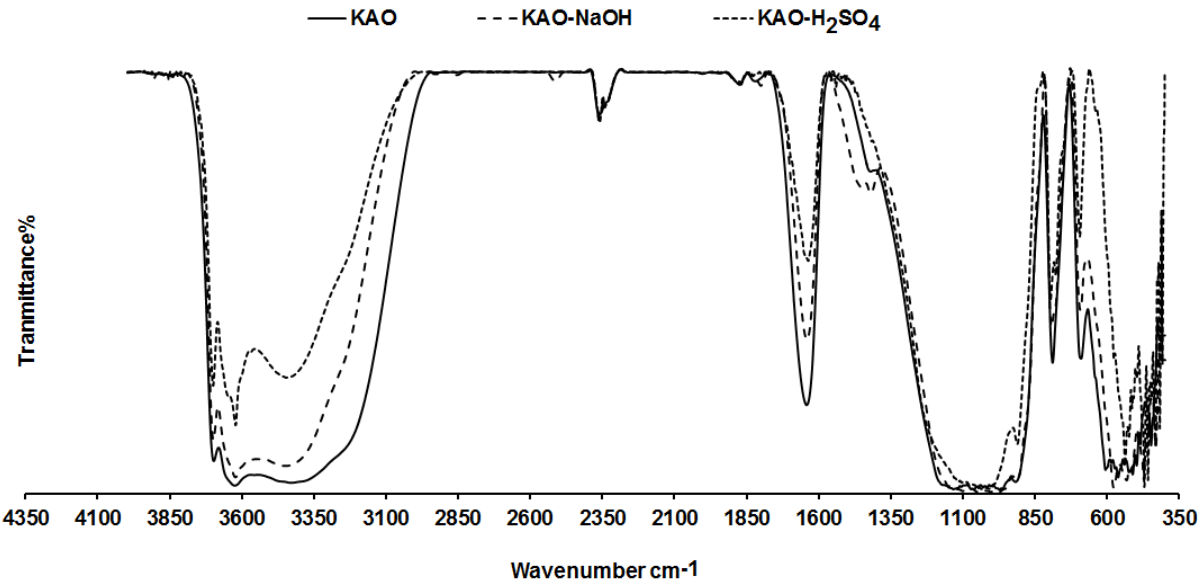

Fig. 3. FTIR spectra of clay samples

[Downloaded from aed.iust.ac.ir on 2025-04-14]

[DOI: 10.22068/ijmse.2114]

Al-OH hydroxyl vibrations were reduced with alkaline treatment, as shown in Fig 3. The materials displayed a number of notable IR bands at 1640, 800, and 700 cm^{-1} in the bending range (400-1650 cm^{-1}).

The bending vibration mode of adsorbed water was blamed for the sharp peak at 1640 cm^{-1} [19]. The bands (800 and 700 cm^{-1}) were assigned to the Al–Al–OH, Al–Mg–OH and Si-O-Al bond vibrations making the sheets the kaolinite clay.

The strong band at 1000-1100 cm^{-1} was attributed to the stretching vibrations of Si-O in kaolinite. IR test indicated the presence of many function groups that would be helpful when explaining the dielectrical characteristics of the samples.

3.2. Dielectrical properties of kaolinitic-clay and modified forms

In general, kaolinite and other modified forms were reported to be good dielectric materials [20, 23]. The dielectric parameters (ac-conductivity, ε', and ε'') were measured as a function of frequency and discussed as following.

AC Conductivity: The relationship between AC conductivity σ_{ac} and the applied frequency (1.0 Hz–10^6 Hz) is provided in Figure 4.

AC conductivity increases with applied frequency for all samples, obviously. In reality, ac affects dielectric polarization and is connected to the imaginary part of epsilon. Several semiconductor materials [23, 38] showed the reported trend (Figure 4A). The relation between σ_{ac} and applied frequency is often described by the following equation [41]: $\sigma_{ac} = A\omega^s$, where A, ω, and s are constant related to the material, angular frequency, and the frequency exponent which is less than or equal unity [41].

The magnitude of s is important as it can reveal the dominant dielectric mechanism. The corresponding values of s which estimated by non-linear regression methodology were, 0.31, 0.35, and 0.36 for KA, KAO-H_2SO_4, and KA-NaOH, respectively. The s values were not falling in the range 0.8-1.0 which exclude the semiconductor nature of the tested materials [23].

The conductivities of samples (at 10 Hz) were 6.36×10^{-9}, 6.69×10^{-8} and 6.87×10^{-8} $(\Omega\ cm)^{-1}$, for KAO-H_2SO_4, KAO, and KAO-NaOH, respectively. As previously stated, acid treatment lowered the initial conductivity by a factor of ten, whereas alkali treatment had no effect on conductivity.

Despite the fact that the conductivity of the studied materials has been much lowered by treatment, they can still be used as semiconductors or insulators with conductivities in the 10-9–10 $(\Omega\ cm)^{-1}$ range. The lower conductivity for KAO-H_2SO^4 would be attributed to serious structural changes and high release of cations as indicated by XRD. Moreover, the higher contents of polar surface groups (Si-OH, Si-O-Si) that generated after acid treatment (See FTIR for samples, Fig 3) had no effect on the electrical conductivity.

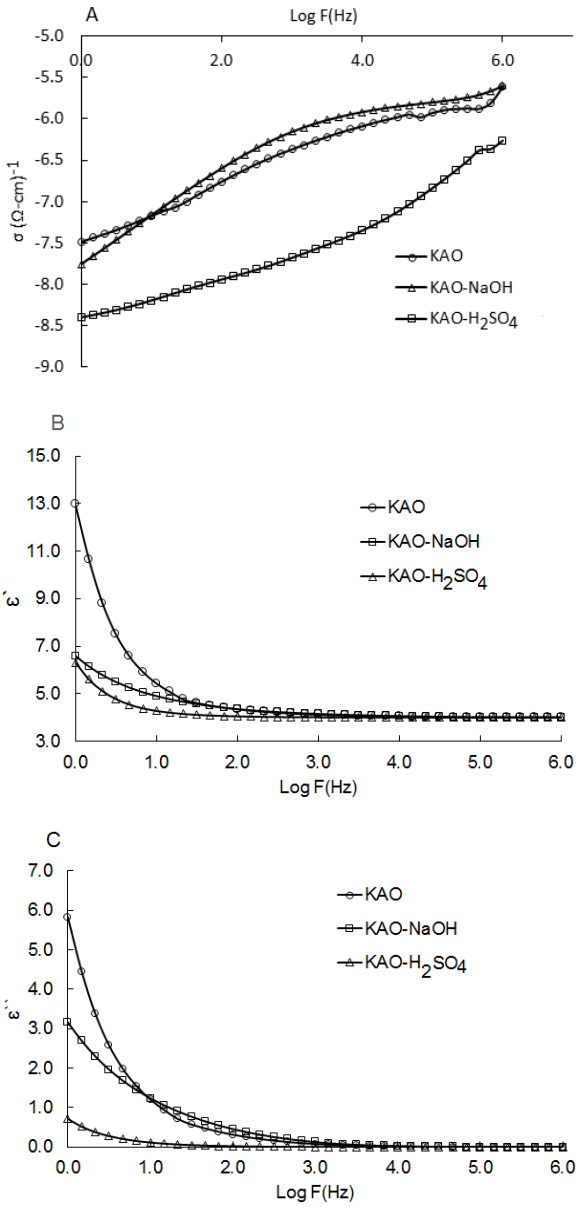

Fig. 4. AC-conductivity A: Dielectric constant B: Dielectric loss factor C as a function of frequency measured at 20°C

[Downloaded from aed.iust.ac.ir on 2025-04-14]

[DOI: 10.22068/ijmse.2114]

Dielectric Constant ε' and Dielectric Loss Constant ε'': For KAO and chemically modified forms, Figure 4B shows the frequency dependence of the dielectric constant ε' (or the real part of the complex dielectric constant). The electric flux density increases as ε' increases, allowing materials to keep their electric charge for longer periods of time or to hold enormous amounts of charge. Materials of high ε' are useful to fabricate high-value capacitors. As shown in Fig 4B, ε' was gradually reduced with frequency and stabilized around 103 Hz for the tested materials. Hence, the studied materials would be used as dielectric materials but at frequencies lower than 103 Hz.

Different polarization processes are observed and dependent on the applied frequency [42]: a) charge polarization 103 Hz, b) dipolar polarization 1010 Hz, c) ionic polarization 1013 Hz, and d) electronic polarization 1016 Hz. Accordingly, the measured process was charge polarization due to impedance mobile charge carries at interfaces within the clay after activation. The electronic, ionic, and orientational relaxations are responsible for the drop in ε' with frequency in ionic and polar materials [41]. In fact, FTIR revealed the polar nature of surface functional groups (Figure 3).

The polar surface groups (Si-OH and Al-OH, see Figure 3) can be polarized via ionic and electronic mechanisms under the strong field and much higher than 106 Hz. It seems that chemical treatment had been altered the structure of raw material as indicated from ε' values in lower-frequency region. For example, at 10 Hz the ε' values were 5.6, 5.1, and 4.1 for KAO, KAO-H_2SO_4, and KAO-NaOH, respectively. The drop in ε' was attributable to the fact that dipoles exposed to an electric field following chemical treatment quickly orient themselves. Simply put, acid and alkali treatments boosted ion-exchange capacity and polar surface functional groups (as validated by FTIR), resulting in greater dipole orientation and improved orientational polarization, resulting in decreased ε'. On the other hand, ε'' (the imaginary part of the complex dielectric constant ε') which corresponds to the dielectric loss of the material was gradually reduced by the applied filed (Figure 4C). Upon application of electric field, the exposed material dissipates a specific quantity of electric energy that converts into heat energy. This process is known as loss of power as the electric power dissipated during a certain interval of time [43, 44]. The frequency-ε'' plots for KAO and chemically modified forms are displayed in Figure 4C.

As illustrated, dielectric loss ε'' is considerable in the low frequency zone (10 Hz) and gradually decreases with applied frequency. At 5.0 Hz, the KAO, KAO-NaOH, and KAO-H_2SO_4 values were 3.3, 2.0, and 0.4, respectively.

Upon chemical treatment, more permanent dipoles will be available, contributing to the polarization as indicated from the higher ε' and ε'' for original sample. Moreover, the increase in ac conductivity of alkali treatment is likely to arise due to the structural changes in KAO network. Based on the ratio ε″/ε′, samples were classified as following [44]: $\varepsilon''/\varepsilon' \ll 1$ the material is a potential dielectric and good conductor at $\varepsilon''/\varepsilon' >> 1$. For a lossy-conducting material, ε″/ε′ is close to unity. The earlier ratio was estimated at different frequencies as shown in Table 2.

As indicated from Table 2, the ratio ε´´/ ε´ was estimated at three regions, low (10 Hz), middle (100 Hz) and high (1000 Hz) to evaluate the dielectrical properties of kaolinite and other treated forms. At low-frequency region, the highest ε´ was reported for KAO (5.42) and this indicated that unmodified materials can concentrate more charge compared to modified forms. Compared to KAO and KAO-H_2SO_4, KAO-NaOH has a much lower dielectric constant (4.31) which reflected it lower polarization when exposed to the electric filed. Similar observation was reported for ε´´ where KAO-NaOH reported to have the lowest dielectric loss factor. At low frequency region, the ratio ε´´/ ε´ revealed that the potential usage of the materials are as dielectrics or insulators. The frequency with which materials are applied is strongly dependent on the frequency with which they are applied, as seen in Table 3.

KAO and KAO-NaOH are potential dielectric materials at 100 Hz, whereas KAO-H_2SO_4 is a common insulator. At much higher frequency (1000 Hz), KAO-H_2SO_4 is a potential dielectric while other forms can be used as insulator. In summary, applicability of tested materials seems to be dependent on the strength of the applied flied.

[Downloaded from aed.iust.ac.ir on 2025-04-14]

[DOI: 10.22068/ijmse.2114]

Table 2. Dielectric parameters reported for kaolinite and other modified forms at variable frequencies to assess their practical applications.

Material	10 Hz				
	ε′	**ε″**	**ε″/ε′**	**Conductivity (Ω cm)$^{-1}$**	**Application**
KAO	5.42	1.21	0.22	6.7×10^{-8}	lossy conducting material good dielectric
KAO-H_2SO_4	5.13	1.12	0.21	6.4×10^{-9}	lossy conducting material good dielectric
KA-NaOH	4.31	0.14	0.03	6.9×10^{-8}	low-conductivity material Insulator
			100 Hz		
KAO	4.42	0.43	0.10	1.7×10^{-7}	lossy conducting material good dielectric
KAO-H_2SO_4	4.34	0.44	0.10	1.1×10^{-8}	low-conductivity material Insulator
KA-NaOH	4.03	0.02	0.005	2.5×10^{-7}	lossy conducting material good dielectric
			1000 Hz		
KAO	4.32	0.16	0.04	4.3×10^{-7}	low-conductivity material Insulator
KAO-H_2SO_4	4.21	0.15	0.04	2.1×10^{-8}	lossy conducting material good dielectric
KA-NaOH	4.04	0.01	0.002	7.0×10^{-7}	low-conductivity material Insulator

Table 3. Potential industrial/environmental applications of clay and chemically-modified forms

Test	Main outputs of the test	Industrial Applications		
		KAO	**KAO-H_2SO_4**	**KAO-NaOH**
XRD and FTIR	-structural changes of kaolinite mineral after acid treatment	Good source for kaolinite/kaolin. Potential adsorbent	Potential adsorbents. Preparation of zeolite from kaolinite upon alkali treatment	
Dielectric parameters	ε′: 4.31-5.42 ε″: 0.14-1.21 conductivity: 6.4×10^{-9}-7.0×10^{-7}	KAO good dielectric at 10 and 100 Hz and insulator at 1000 Hz	KAO-H_2SO_4 good dielectric at 10 and 1000 Hz and insulator at 100 Hz	KAO-NaOH good insulator at 10 and 1000 Hz and good dielectric at 100 Hz
Shielding parameters (at 10 keV)	mass attenuation coefficient (μ/ρ): 12.098-12.182 cm^2/g *Half value layer*: 10 cm	Potential usage as shielding materials for Gamma ray		

3.3. Shielding properties of clay samples

The intensity of gamma-photons is attenuated when they pass through a clay sample of thickness (t), and this attenuation is represented by Beer-law, Lambert's which is [25, 29, 31]:

$$I = I_o e^{-\mu t} \quad (1)$$

where I and I_0 denote the photons intensity after

[Downloaded from aed.iust.ac.ir on 2025-04-14]

[DOI: 10.22068/ijmse.2114]

and before passing the clay sample, and μ represents the linear attenuation coefficient (cm^{-1}) of the clay sample. The μ expresses the fraction of a beam of gamma photon which scattered or absorbed per unit thickness of the sample. μ values depend on the composition of the samples, the energy of the incident photon, the thickness and the density of the sample [24, 25]. The mass attenuation coefficient (μ/ρ, cm^2/g) is another important parameter that can be used to evaluate the gamma photons shielding characterization for the present clay samples. For the selected clay samples, the μ/ρ is the sum of the elements that made up the samples (i.e Si, Al, Fe, K, etc). Therefore, the μ/ρ of each sample can be calculated using Bragg`s law [45]:

$$(\mu/\rho)_{clay} = \sum_i^n w_i \left(\frac{\mu}{p}\right)_i \quad (2)$$

where w is the mass fraction of the components that make up the clay (Si, Al, Fe, etc) (Table 2). The μ/ρ values of the elements constituting the clay at different energy values (between 0.015-15 MeV or 15-15,000 keV) were obtained from XCOM program as outlined in the literature [25, 45]. The μ/ρ values of clay samples at twenty-six gamma energies were estimated and presented in Figure 5.

The change in μ/ρ with the energy presented in Fig 5, in fact, is in accordance with that reported in the literature for common clay-materials including Kaolin and Ball clay [21]. Also, the μ/ρ trend presented in Fig 5A is in line with the work achieved by Mann and co-researchers who studied the gamma radiation attenuation features for some burnt clay bricks between 0.001–15 MeV [45]. As indicated in Fig 5A and for all samples, μ/ρ was found to decrease rapidly with the increase in the energy at the beginning, and decreases more gradually between 0.05-3 MeV. The photoelectric absorption, which is the main interaction between low-energy photons and all kaolinitic materials, is likely to be the cause of such a large decrease in μ/ρ at first. The μ/ρ for all clays decrease slowly between 0.05-3.0 MeV since the Compton scattering is the primary interaction mechanisms between photons with such energies with the clay samples [46-48]. Furthermore, for all samples (12.098, 12.121, and 12.182 cm^2/g for KAO, KAO-H_2SO_4, and KAO-NaOH, respectively), the value of μ/ρ has the maximum value of 0.015 MeV. Such high magnitude at low energy is due to the fact that the probability for the photoelectric absorption to occur varies with the atomic number as Z^{4-5}. Moreover, chemical treatment did not affect the corresponding μ/ρ values and hence all samples have comparable shielding properties. Z_{eff} value: One of the nuclear parameters that must be evaluated to choose and design appropriate shielding materials is the effective atomic number (Z_{eff}).

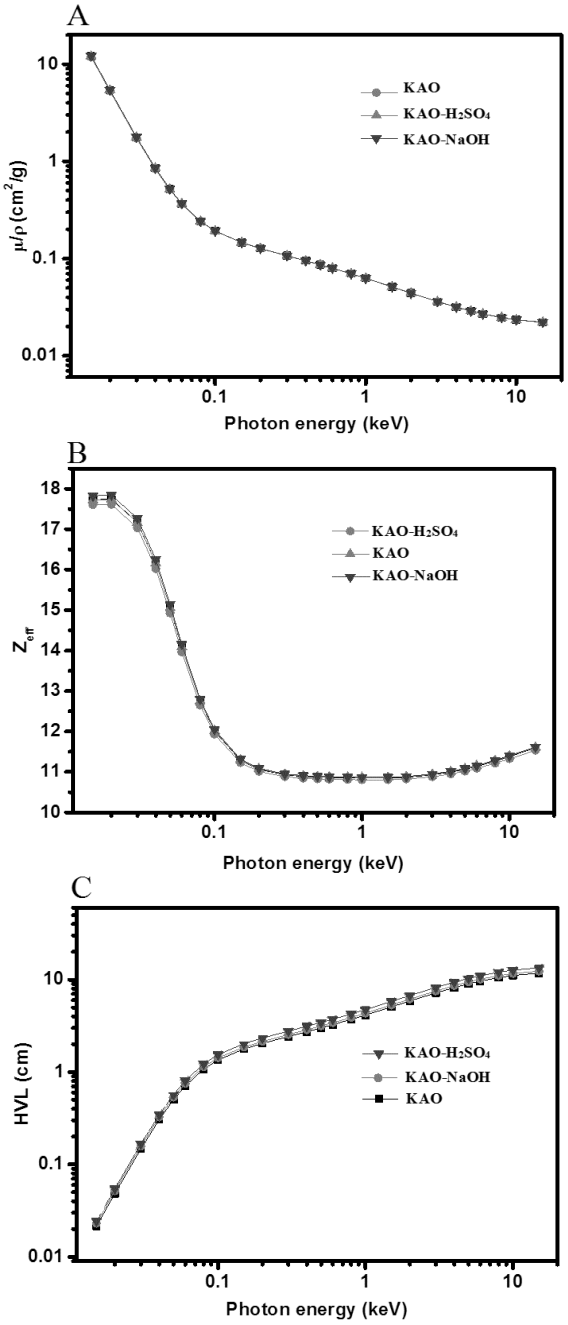

Fig. 5. Shielding parameters of kaolinitic samples estimated at 0.015-15 MeV for kaolinitic samples. Mass attenuation coefficients A: Effective atomic number B: Half value layer C

[Downloaded from aed.iust.ac.ir on 2025-04-14]

[DOI: 10.22068/ijmse.2114]

The Z_{eff} of the clays under investigation was calculated using the following equation [29, 49]:

$$Z_{eff} = \frac{\sum_i f_i A_i \left(\frac{\mu}{\rho}\right)_i}{\sum_j f_j \frac{A_j}{Z_j} \left(\frac{\mu}{\rho}\right)_j} \quad (3)$$

Where f_i is the fractional abundance of the element i. The corresponding Z_{eff} curve as a function of the energy for all investigated clays is exhibited in Fig 5B. Z_{eff} appears to have the highest E0.1 MeV values for all clays examined (photoelectric region). The Z_{eff} of the drops fast with increasing energy up to 0.2 MeV, as seen by the Z_{eff} graph. Z_{eff} values are nearly consistent between 0.3 keV and 15 MeV. Because of the low percentage of Ca following acid treatment, KAO-HCL has the lowest Z_{eff}.

3.3.1. Half value layer

The half value layer (HVL) is a valuable metric in the design and selection of any photon attenuation material since it represents the material thickness necessary to reduce the radiation intensity to 50% of its original value [50]. The less HVL value, the better the attenuation properties it possess. The HVL is inversely proportional to the linear attenuation coefficient and estimated for clay samples as [39, 29]:

$$HVL = \frac{0.693}{\mu} \quad (4)$$

The HVL results of the tested clays at several photon energies are plotted and given in Fig 5C. The results showed a relationship between the density of the clay and the absorption capacity of the sample. The estimated densities of the raw and treated samples were 2.664, 2.332 and 2.132 g/ml for KAO, KAO-NaOH and KAO-H_2SO_4, respectively. Lower densities were expected upon treatment especially in HCl case. The higher the density, the lower the HVL, indicating that the high density clay sample had a beneficial impact on the sample's absorption capabilities. On the other hand, it is possible to deduce that an increase in density resulted in a decrease in the thickness of the clay shield. As indicated in Fig 5C, KAO exhibited lower HVL particularly at higher photon energy while acid-treated clay has a longer HVL value. Moreover, HVL increases with the increase in the energy, which indicated that the low energy photons need a shorter distance to lose their energy, whereas high energy can lose their energy in a longer distance. As a result of this finding, it may be concluded that untreated clay is better suited to shielding high-energy photons than chemically treated clay. When compared to Ag-containing glass (2.5 cm^2/g) and regular concrete (4.5 cm^2/g), the measured HVL of the tested materials was closed to 3.0 cm^2/g at 1.0 ke, which appears to be an adequate shielding medium [29].

3.4. Potential applications of kaolinite and treated forms

The practical applications of clay and other modified forms samples would be judged depending on the outputs of characterization tests. The potential industrial applications of the materials are provided in Table 3.

XRD indicated the high content of kaolinite in the raw sample. Upon treatment, XRD indicated serious structural changes by H_2SO_4 and formation of zeolite upon NaOH treatment. IR indicated the presence of polar functional groups which support the application of the materials as adsorbents. All of the samples had a Si/Al ratio of less than 3.0, indicating that they might be used to make geopolymers. Dielectric studies also revealed that the materials could be used as a dielectric or an insulator, depending on the applied frequency. Analysis also indicated that all materials are poorly conductors. For example, KAO-H_2SO_4 is a good dielectric material at 10 and 1000 Hz but can be used as insulator at 100 Hz. Finally, kaolinite and other treated forms are adequate shielding materials with high mass attenuation coefficients (μ/ρ) 12.098-12.182 cm^2/g reported at 10 keV.

4. CONCLUSIONS

The outcome of adopted characterization tests were rather useful to decide the proper practical application of the studied samples. Analysis indicated that natural sample has high kaolinite (51%) content which is necessary for kaolin production. Furthermore, XRD revealed that acid treatment resulted in structural deformation of kaolinite while alkali treatment resulted in a phase change into zeolite. XRF revealed that Al and Fe released more energy than Si, and that the changed materials may be used in the synthesis of geopolymers (Si/Al ratio 1.5– 2.0). KAO-H_2SO_4 was shown to be a suitable dielectric material in the low frequency range (10-1000 Hz). All materials exhibited a high shielding efficiency as deduced from the high mass attenuation coefficients.

[Downloaded from aed.iust.ac.ir on 2025-04-14]

[DOI: 10.22068/ijmse.2114]

5. ACKNOWLEDGMENTS

The authors wish to thank the Faculty of Graduate Studies and Research/Hashemite University for the financial support. Technical assistance by Mr. Bassem Nasrallah is highly appreciated.

REFERENCES

[1] Leluk, K., Orzechowski, K., Jerie, K., Baranowski, A., Sonka, T. and Gowinski J. "Dielectric permittivity of kaolinite heated to high temperatures." J. Phy.Chem. Solid 2010, 71, 827–831.

[2] Ramesh, S., Bhati, Y.S. and Jai Prakash, B.S., "Microwave-activated p-TSA dealuminated montmorillonite—a new material with improved catalytic activity." Clay Minerals 2012, 47, 231–242.

[3] Kooli, F., Liu, Y., Al-Faze, R. and Al Suhaimi A., "Effect of acid activation of Saudi local clay mineral on removal properties of basic blue 41 from an aqueous solution." Appl. Clay Sci. 2015, 116, 23–30.

[4] Komadel P., "Acid activated clays: Materials in continuous demand." Appl. Clay Sci. 2016, 131, 84-99.

[5] Jozefaciuk G., "Effect of acid and alkali treatments on surface charge properties of selected minerals." Clays and Clay Miner. 2002, 50, 647–656.

[6] Belver, C., Munoz, M. and Vicente, M., "Chemical Activation of a Kaolinite under Acid and Alkaline Conditions." Chem. Mater. 2002, 14, 2033-2043.

[7] Hussin, F., Aroua, M.K. and Daud, W.M., "Textural characteristics, surface chemistry and activation of bleaching earth: A review" Chem. Eng. J. 2011, 170, 90–106.

[8] Wang, Q., Zhang, J.P., Zheng, Y. and Wang, A.Q., "Adsorption and release of ofloxacin from acid- and heat-treated halloysite." Colloid Surf. B: Biointerfac. 2014, 113, 51–58.

[9] Korichi, S., Elias, A. and Mefti, A., "Characterization of smectite after acid activation with microwave irradiation." Appl. Clay Sci. 2009, 42, 432–438.

[10] Al-Bakain, R.Z., Al-Degs, Y.S., Issa, A.A., Jawad, S.A. and Abu Safieh K.A., "Activation of kaolin with minimum solvent consumption by microwave heating." Clay Mine. 2014, 49, 667–681.

[11] Wu Z., Li C., "Kinetics and thermodynamics of carotene and chlorophyll adsorption onto acid-activated bentonite from Xinjiang in xylene solution." J. Hazard. Mater. 2009, 171, 582–587.

[12] Caglayan, M.O., Kafa, S. and Yigit, N., "Al-pillared clay for cottonseed oil bleaching: an optimization study." J. Amer. Oil Chem. Soc. 2005, 82, 599–602.

[13] Gunawan, N.S., Indraswati, N., Ju Y.H., Soetaredjo, F.E., Ayucitra, A., and Ismadji, S., "Bentonites modified with anionic and cationic surfactants for bleaching of crude palm oil." Appl. Clay Sci. 2010, 47, 462–464.

[14] Provis J.L. "Geopolymers and other alkali activated materials: why, how, and what? Materials and Structures 2014, 47, 11–25.

[15] Alastair, M., Andrew H., Pascaline, P., Mark, E. and Pete W., "Alkali activation behaviour of un-calcined montmorillonite and illite clay minerals." Appl Clay Sci. 2018, 166, 250–261.

[16] Heller-Kallai, L. and Lapides I., "Reactions of kaolinites and metakaolinites with NaOH—comparison of different samples (Part 1). Appl. Clay Sci. 2007, 35, 99–107.

[17] Liew, Y.M., Heah, C.Y., Mohd Mustafa, A.B. and Kamarudin, H., "Structure and properties of clay-based geopolymer cements: a review." Prog. Mater. Sci. 2016, 83, 595–629.

[18] Duxson, P., Fernández-Jiménez, A., Provis, J.L., Lukey, G.C., Palomo, A., and van Deventer, J., "Geopolymer technology: the current state of the art." J. Mater. Sci. 2007, 42, 2917–2933.

[19] Kumar, S., Panda A. and Singh R., "Preparation and characterization of acids and alkali treated kaolin clay." Bull. Chem. Reac. Eng. & Catal. 2013, 8, 61–69.

[20] Orzechowski, K., Słonka, T. and Głowinski, J., "Dielectric properties of intercalated kaolinite." J. Phys. Chem. Solid 2006, 67, 915-919.

[21] Olukotun, S.F., Gbenu, S.T., Ibitoye, F.I., Oladejo, O.F., Shittu, H.O., Fasasi, M.K. and Balogun, F.A., "Investigation of gamma radiation shielding capability of

[Downloaded from aed.iust.ac.ir on 2025-04-14]

[DOI: 10.22068/ijmse.2114]

two clay materials." Nuc. Eng. Technol. 2018, 50, 957-962.

[22] Rahman, M.M., "Magnetic and dielectric properties of materials: Basics, theories and experiments paperback. 2012 LAP LAMBERT Academic Publishing. 2012.

[23] Salman, F.E. and Mekki, A., "Dielectric study and ac conductivity of iron sodium silicate glasses." J. Non-Crystall. Solid 2011, 357, 2658–2662.

[24] Akbulut, S., Sehhatigdiri, A., Eroglu, H. and Çelik, S., "A research on the radiation shielding effects of clay, silica fume and cement samples." Rad. Phys. Chem. 2015, 117, 88–92

[25] Al-Buriahi, M., Barıs, H., and Tonguç, B., "Mass attenuation coefficients, water and tissue equivalence properties of some tissues by Geant4, XCOM and experimental data." Indian J. Pure Appl. Phys. 2019, 57, 433–437.

[26] Al-Buriahi, M. and Mann, K. "Radiation shielding investigations for selected tellurite-based glasses belonging to the TNW system." Mater. Res. Expr. 2019, 6, 105206

[27] Tajudin, S., Sabri, A., Abdul Aziz, M., Olukotun, S., Ojo, B. and Fasasi, M. "Feasibility of clay-shielding material for low-energy photons (Gamma/X)." Nuc. Eng. Techno. 2019, 51, 1633-1637.

[28] Al-Buriahi, M., Bakhsh E., Tonguc B. and Khan. S., "Mechanical and radiation shielding properties of tellurite glasses doped with ZnO and NiO." Ceram. Inter. 2020, 46, 19078–19083.

[29] Al-Buriahi, M., Somaily, H., Alalawi, A., Alraddadi, and S. Polarizability, "Optical Basicity, and Photon Attenuation Properties of $Ag_2O–MoO_3–V_2O_5–TeO_2$ Glasses: The Role of Silver Oxide." J. Inorg. Organometall. Polym. Mater. 2020 (doi.org/10.1007/s10904-020-01750-z)

[30] Al-Buriahi and M., Singh, V. "Comparison of shielding properties of various marble concretes using GEANT4 simulation and experimental data." J. Aust. Ceram. Soc. 202, 56, 1127–1133.

[31] Hegazy, H., Al-Buriahi, M., Alresheedi, F., El-Agawany, F., Sriwunkum, C. Neffati, R., and Rammah, Y. "Nuclear shielding properties of $B_2O_3–Bi_2O_3–SrO$ glasses modified with Nd_2O_3: Theoretical and simulation studies." Ceram. Inter. 2021, 47, 2772-2780.

[32] Olarinoye, I., Alomairy, S., Sriwunkum, C., and Al-Buriah, M. "Effect of Ag_2O/V_2O_5 substitution on the radiation shielding ability of tellurite glass system via XCOM approach and FLUKA simulations." Physica Scripta 2021, 96, 6, 065308.

[33] Alzahrani, J., Alothman, M., Eke, C., Al-Ghamdi, H., Aloraini, D., Al-Buriahi, M., "Simulating the radiation shielding properties of $TeO_2–Na_2O–TiO$ glass system using PHITS Monte Carlo code." Computational Materials Science 2021, 196, 110566.

[34] Kebaili, I., Znaidia, S., Alzahrani, J., Alothman, M., Boukhris, I., Olarinoye, I., Mutuwong, C., Al-Buriahi, M., "Ge 20 Se 80-x Bi x (x≤ 12) chalcogenide glasses for infrared and gamma sensing applications: structural, optical and gamma attenuation aspects." J. Mater. Sci.: Mater. Electron. 2021, 32, 15509–15522.

[35] Al-Buriahi, M., Bakhsh, E., Tonguc, B., Khan, S. "Mechanical and radiation shielding properties of tellurite glasses doped with ZnO and NiO." Ceramics International 46, no. 11 (2020): 19078-19083.

[36] A. Mefire, R. Fouateu, A. Njoya, J. Mache, P. Pilate, F. Hatert, N. Fagel. "Mineralogy and geochemical features of Foumban clay deposits (west Cameroon): genesis and potential applications." Clay Miner. 2018, 53, 431 – 445.

[37] Panda, A.K., Mishra, B.G., Mishra, D.K., and Singh, R.K., "Effect of sulphuric acid treatment on the physico-chemical characteristics of kaolin clay." Colloid. Surf. A: Physicochem. Eng. Aspec. 2010, 363, 98-104

[38] Attia, A.A., Soliman, H.S., Saadeldin, M.M., and Sawaby, K., "AC electrical conductivity and dielectric studies of bulk p-quaterphenyl." Synth. Metal. 2015, 205, 139–144.

[39] Pentrak, M., Madejova, J., and Komadel, P., "Acid and alkali treatment of kaolins." Clay Miner. 2009, 44, 511–523.

[40] Jozefaciuk, G., and Bowanko G., "Effect of

[Downloaded from aed.iust.ac.ir on 2025-04-14]

[DOI: 10.22068/ijmse.2114]

acid and alkali treatments on surface areas and adsorption energies of selected minerals." Clays Clay Miner. 2002, 50, 771–783.

[41] Afifi, M.A., Bekheet, A.E., Abd Elwahhab, E., and Atyia H.E., "Ac conductivity and dielectric properties of amorphous In_2Se_3 films." Vacuum 2001, 61, 9-17.

[42] Loewer, M., Günther, T., Igel, J., Kruschwitz, S., Martin, T., and Wagner, N., "Ultra-broad-band electrical spectroscopy of soils and sediments—a combined permittivity and conductivity model." Geophy. J. Inter. 2017, 210, 1360–1373

[43] Bekheet, A., and Hegab, N.A., "Ac conductivity and dielectric properties of $Ge_{20}Se_{75}In_5$ films." Vacuum 2008, 83, 391-396.

[44] Magee, T., McMinn, W., Farrell, G., Topley, L., Al-Degs, Y.S., Walker, G., and Khraisheh M., "Moisture and temperature dependence of the dielectric properties of pharmaceutical powders. J. Therm. Anal. Calorim. 2013, 111, 2157–2164.

[45] Singh, V.P. Badiger, N.M., and Kucuk, N., "Gamma-ray and neutron shielding properties of some soil samples. Indian J. Pure Appl. Phys. 2014, 52, 579-587.

[46] Mann, H.S., Brar, G., Mann, K., and Mudahar, G., "Experimental Investigation of Clay Fly Ash Bricks for Gamma-Ray Shielding." Nuc. Eng. Technol. 2016, 48, 1230 -1236.

[47] Mann, K.S., Heer, M.S., and Rani, A., "Investigation of clay bricks for storage facilities of radioactive-wastage, Appl. Clay Sci. 2016, 119, 249–256.

[48] Gaikwad, D.K., Sayyed, M.I., Obaid, S.S., Issa S.A., and Pawar P.P., "Gamma ray shielding properties of TeO_2-ZnF_2-As_2O_3-Sm_2O_3 glasses." J. Alloys Compound. 2018, 765, 451-458.

[49] Lakshminarayana, G., Kumar, A., Dong, M.G., Sayyed, M.I., Long, N., and Mahdi M.A., "Exploration of gamma radiation shielding features for titanate bismuth borotellurite glasses using relevant software program and Monte Carlo simulation code." J. Non-Cryst. Solid 2018, 481, 65–73

[50] Agar, O., Khattari, Z.Y., Sayyed, M.I., Tekin, H.O., Al-Omari, S., Maghrabi, M., Zaid, M.H., and Kityk I.V., "Evaluation of the shielding parameters of alkaline earth based phosphate glasses using MCNPX code." Result Phys. 2019, 12, 101–106.

[Downloaded from aed.iust.ac.ir on 2025-04-14]

[DOI: 10.22068/ijmse.2114]